



The effects of technological voids on the hydro-mechanical behaviour of compacted bentonite-sand mixture

Qiong Wang, Anh Minh A.M. Tang, Yu-Jun Cui, Pierre Delage,
Jean-Dominique Barnichon, Wei-Min Ye

► To cite this version:

Qiong Wang, Anh Minh A.M. Tang, Yu-Jun Cui, Pierre Delage, Jean-Dominique Barnichon, et al.. The effects of technological voids on the hydro-mechanical behaviour of compacted bentonite-sand mixture. *Soils and Foundations*, 2013, 53 (2), pp.232-245. 10.1016/j.sandf.2013.02.004 . hal-00829480

HAL Id: hal-00829480

<https://hal-enpc.archives-ouvertes.fr/hal-00829480>

Submitted on 3 Jun 2013

HAL is a multi-disciplinary open access archive for the deposit and dissemination of scientific research documents, whether they are published or not. The documents may come from teaching and research institutions in France or abroad, or from public or private research centers.

L'archive ouverte pluridisciplinaire **HAL**, est destinée au dépôt et à la diffusion de documents scientifiques de niveau recherche, publiés ou non, émanant des établissements d'enseignement et de recherche français ou étrangers, des laboratoires publics ou privés.

The effects of technological voids on the hydro-mechanical
behaviour of compacted bentonite-sand mixture

Qiong Wang¹, Anh Minh Tang¹, Yu-Jun Cui^{1,3}, Pierre Delage¹, Jean-Dominique
Barnichon², Wei-Min Ye³

¹ *Ecole des Ponts ParisTech, Navier/CERMES¹, France*

² *Institut de Radioprotection et de Sûreté Nucléaire (IRSN), France*

³ *Tongji University, China*

Corresponding author:

Prof. Yu-Jun CUI

Ecole des Ponts ParisTech

6-8 av. Blaise Pascal, Cité Descartes, Champs-sur-Marne

77455 MARNE LA VALLEE

France

Telephone : +33 1 64 15 35 50

Fax : +33 1 64 15 35 62

E-mail : yujun.cui@enpc.fr

¹ Centre d'Enseignement et de Recherches en Mécanique des Sols

Abstract

Compacted bentonite-based materials are often used as buffer materials in radioactive waste disposal. A good understanding of their hydro-mechanical behaviour is essential to ensure the disposal safety. In this study, a mixture of MX80 bentonite and sand was characterized in the laboratory in terms of water retention property, swelling pressure, compressibility and hydraulic conductivity. The effects of the technological voids or the voids inside the soil were investigated. The technological voids are referred to as the macro-pores related to different interfaces involving the buffer material, whereas the voids inside the soil is referred to as the common macro-pores within the compacted bentonite/sand mixture. The results obtained show that at high suctions, the amount of water absorbed in the soil depends solely on suction, whereas at low suctions it depends on both suction and bentonite void ratio. There is a unique relationship between the swelling pressure and the bentonite void ratio, regardless of the sample nature (homogeneous or not) and sand fraction. However, at the same bentonite void ratio, a higher hydraulic conductivity was obtained on the samples with technological voids. The effect of sand fraction was evidenced in the mechanical yield behaviour: at the same bentonite void ratio, the bentonite-sand mixture yielded at a higher pre-consolidation stress.

Keywords: Bentonite-sand mixture; Technological voids effects; Water retention property; Swelling pressure; Hydraulic conductivity; Compressibility.

1 INTRODUCTION

Most designs of deep geological repository for high level radioactive wastes (HLW) are based on the multi-barrier concept with isolation of the waste from the environment. The multi-barrier concept includes the natural geological barrier (host rock), engineered barriers made up of compacted sand-bentonite mixtures (placed around waste containers or used as buffer and sealing elements) and metal canister. Compacted bentonite-based materials are relevant materials for this purpose thanks to their low permeability, high swelling and high radionuclide retardation capacities (Pusch, 1979; Yong et al., 1986; Villar and Lloret, 2008; Komine and Watanabe, 2010; Cui et al., 2011).

Engineered barriers are often made up of compacted bricks. When bricks are placed around waste canisters or to form sealing buffers, the so-called technological voids either between the bricks themselves or between bricks, canisters and the host rock are unavoidable. As an example, 10 mm thick gaps between bentonite blocks and canister and 25 mm thick gaps between the bentonite blocks and the host rock have been considered in the basic design of Finland (Juvankoski, 2010). These technological voids appeared to be equal to 6.6 % of the volume of the gallery in the

66 FEBEX mock-up test (Martin et al., 2006). Fractures that appear in the excavation
67 damaged zone within the host rock in the near field constitute additional voids. In the
68 French concept, the volume of the bentonite/rock gaps is estimated at 9 % of the
69 volume of the gallery by the French waste management agency (ANDRA 2005). This
70 value reaches 14 % in the SEALEX in-situ test carried out in the Tournemire
71 Underground Research Laboratory (URL) run by IRSN (Institut de radioprotection et
72 de sûreté nucléaire, the French expert national organisation in nuclear safety) in
73 South-West of France (Barnichon and Deleruyelle, 2009).

74 Once placed in the galleries, engineered barriers are progressively hydrated by pore
75 water infiltrating from the host-rock. This water infiltration is strongly dependent on
76 the initial state of the compacted material (water content, suction and density, e.g. Cui
77 et al. 2008). Indeed, it has been shown that water transfer in unsaturated swelling
78 compacted bentonites or sand bentonite mixtures is strongly dependent on the
79 imposed boundary conditions in terms of volume change. As shown in Yahia-Aissa et
80 al. (2001), Cui et al. (2008) and Ye et al. (2009), the degree of swelling allowed
81 significantly affects the amount of infiltrated water, with much water absorbed when
82 swelling is allowed and a minimum amount of water absorbed when swelling is
83 prevented. Volume change conditions also appeared to have, through microstructure
84 changes, significant influence on the hydraulic conductivity.

85 In this regard, the degree of swelling allowed by the technological voids described
86 above has a significant influence on the hydro-mechanical behaviour of the
87 compacted bentonite and their effects need to be better understood. Swelling results in
88 a decrease in dry density that may lead to a degradation of the hydro-mechanical
89 performance of engineered barriers (Komine et al., 2009, Komine, 2010). As a result,
90 the safety function expected in the design may no longer be properly ensured.
91 Therefore, a better understanding of the effects of the technological voids is essential
92 in assessing the overall performance of the repository.

93 In this study, a series of tests was performed on a compacted bentonite-sand mixture
94 samples, aiming at investigating the effects of technological voids on their
95 hydro-mechanical behaviour. Temperature effects were not considered and tests were
96 carried out at constant ambient temperature ($20\pm1^{\circ}\text{C}$). Given that the paper deals with
97 the hydration of engineered barriers in the repository, neither the drying process nor
98 hysteresis effects were considered.

99 Firstly, the water retention curve was determined under both free swell and restrained
100 swell conditions; secondly, the effects of a pre-existing technological void on both the
101 swelling pressure and hydraulic conductivity were investigated; finally, the
102 compressibility at different void ratios was studied by means of suction-controlled
103 oedometer tests. An overall analysis of the effects of voids on the hydro-mechanical
104 response of the engineered barrier was finally performed.

2 MATERIALS AND METHODS

2.1 Materials and sample preparation

A commercial MX80 Na-bentonite from Wyoming, USA was used. The bentonite powder was provided with an initial water content of 12.2% and was stocked in a hermetic container to maintain the water content constant, in a room at $20\pm 1^\circ\text{C}$. All tests were performed at this temperature.

This MX80 Na-bentonite is characterised by a high montmorillonite content (80%), a liquid limit of 575%, a plastic limit of 53% and a unit mass of the solid particles of 2.77 Mg/m^3 . The cation exchange capacity (CEC) is 76 meq/100g (83 % of Na). The grain size distribution (Figure 1) determined using a hydrometer (French standard AFNOR NF P94-057) on deflocculated clay shows that the clay fraction ($< 2 \mu\text{m}$) is 84%. The X-Ray diffractometer diagram of the clay fraction presented in Figure 2 shows a peak at 12.5 \AA , typical of montmorillonite (this peak shifted from 12.5 to 16.9 \AA when treated with glycol and to 9.5 \AA when dried). These data are comparable with that provided by Montes-H et al., (2003).

The sand used in the mixture was a quartz sand from the region of Eure and Loire, France, that passed through a 2 mm sieve. Figure 1 shows the sand grain size distribution curve determined by dry sieving (AFNOR NF P94-056). The curve is characterized by a uniformity coefficient C_u of 1.60 and a D_{50} close to 0.6 mm. The unit mass of the sand grains is 2.65 Mg/m^3 .

A water having the same chemical composition as the pore water of the Callovo-oxfordian claystone from the ANDRA URL in Bure (France), called synthetic water, was used in the experiments. The corresponding chemical components (see Table 1) were mixed with distilled water in a magnetic stirrer until full dissolution.

The grain size distribution of the bentonite powder obtained by “dry” sieving is also presented in Figure 1, showing a well graded distribution around a mean diameter slightly larger than 1 mm. This curve is close to that of sand. The powder was carefully mixed with dry sand (70% bentonite - 30% sand in mass) giving a water content of 8.5% for the mixture. Prior to compaction, the mixture powder was put into a hermetic container connected to a vapor circulation system (see Figure 3) containing free water (100% relative humidity), so as to reach a target water content of 11%. The samples were weighed every two hours until the target water content was attained (after around two days).

A given quantity of mixture was then placed into a rigid ring (35 or 38 mm diameter) and statically compacted using an axial press at a constant displacement rate of 0.05 mm/min to different target dry densities (values given in the following section). Once the target dry density reached, the displacement shaft was fixed for more than

15 h to attain axial stress stabilization (defined by changes in axial stress as low as 0.05 MPa/h). This procedure minimized the sample rebound during unloading.

The results from Mercury intrusion porosimetry (MIP) tests on the bentonite/sand mixtures compacted to dry densities $\rho_d = 1.67$ and 1.97 Mg/m^3 and freeze dried are shown in Figure 4. A typical bimodal porosity (e.g. Ahmed et al. 1974, Delage et al. 1996, Romero et al. 1999) was observed in both samples, defining intra-aggregate pores (micro-pores) with a mean size of $0.02 \text{ }\mu\text{m}$ and inter-aggregate pores (macro-pores) that depend on the dry density and range from $10 \text{ }\mu\text{m}$ (for $\rho_d = 1.67 \text{ Mg/m}^3$) to $50 \text{ }\mu\text{m}$ ($\rho_d = 1.97 \text{ Mg/m}^3$). As shown by Delage and Graham (1995) from the data of Sridharan et al. (1971), this confirms that compaction only affects the largest inter-aggregate pores while intra-aggregate pores remain unaffected (see also Lloret and Villar, 2007). In compacted bentonites, it has been shown that a further smaller sized pore population (ranging between 0.2 and 2 nm) corresponding to the intra-particle (interlayer) pores within the aggregates and not detectable by the MIP had to be also considered (Delage et al., 2006; Lloret and Villar, 2007).

2.2 Experimental methods

2.2.1 Water retention test

The water retention curve (WRC) of the bentonite/sand mixture was determined under both free swell and restrained swell conditions by using both the vapour equilibrium technique ($s > 4.2 \text{ MPa}$) and osmotic technique ($s < 4.2 \text{ MPa}$) for suction control. Three identical samples were used in parallel and the final water content calculated corresponds to the mean value. To apply suction by the vapour equilibrium technique under free swell conditions the as-compacted sample (35 mm diameter and 5 mm height) was placed into a desiccator containing a saturated salt solution at bottom. The sample mass was regularly measured to monitor the water content variation over time. In a standard fashion, equilibrium was considered reached when the mass stabilized. To apply the osmotic technique (Delage et al. 1998; Delage and Cui, 2008a and 2008b), the sample was wrapped by a cylinder-shaped semi-permeable membrane and placed in a PEG 20 000 solution at a concentration corresponding to the required suction. The water content at equilibrium under each suction was determined by weighing.

Following Yahia-Aissa et al. (2001), the determination of the water retention curve under prevented swell conditions (constant volume conditions) was carried out on samples of 50 mm in diameter and 5 mm in height, placed into a specially designed rigid stainless steel cell allowing vapour exchanges through two metal porous disks put on both sides. To apply the osmotic technique, the semi-permeable membrane was placed between the porous stone and the soil sample (Figure 5a); all was then sandwiched between two perforated discs and immersed into a PEG solution at the required concentration. Water infiltrated into the soil through the porous stone and the

semi-permeable membrane until the target suction was reached. To apply suction with the vapour equilibrium technique, the sample sandwiched between two porous stones was installed between two external plates with valves (Figure 5b) that were connected to a suction control system using the vapour equilibrium technique. The water content at equilibrium under each suction was determined by weighing.

All the tests performed and the solutions used for suction control (Delage et al., 1998; Ye et al., 2009) are presented in Table 2. Samples were statically compacted at a dry density of 1.67 Mg/m^3 , corresponding to the final dry density adopted in the in situ experiment at the Tournemire URL.

2.2.2 Hydration test with technological void (SP 01 - 04)

The effect of technological void on the swelling behaviour of the compacted sand-bentonite mixture was investigated using the device shown in Figure 6. In this system, a sample is placed inside an oedometer cell placed into a rigid frame comprising a load transducer that allows the measurement of vertical stress during hydration. The small vertical strain due to the deformability of the set-up is measured by a digital micrometer.

A technological void of 14% of the total cell volume that corresponds to the situation of the SEALEX in situ test at the Tournemire URL was set by choosing an initial diameter of the compacted sample smaller than that of the hydration cell. With a ring diameter of 38 mm, the annular technological void selected (14% of the total cell volume representing 17% of the initial sample volume) corresponded to a sample diameter of 35.13 mm.

The sample was hydrated by injecting synthetic water under constant pressure (0.1 MPa) through a porous disk in contact with the bottom face while the top face was put in contact with another porous stone so as to allowed free expulsion of either air or water (see Figure 6). The small water pressure (0.1 MPa) was adopted to avoid any effect on axial pressure measurement. Changes in axial stress, displacement and injected water volume over time were monitored. Once the axial stress stabilized (after more than 35 h, see Figure 9), water injection under 0.1 MPa was continued for 24 h more in order to determine the hydraulic conductivity under permanent flow condition. Indeed, a linear relationship between flux and time was observed, confirming the observation of Dixon et al. (1992) about the validity of Darcy's law for saturated compacted bentonites.

Four tests with the same technological void of 14% (SP01 - SP04) were conducted on samples with the same initial water content of 11% and various initial dry densities obtained by changing the compaction pressure (between 65 and 85 MPa, giving rise to dry densities comprised between 1.93 and 1.98 Mg/m^3 , see Table 3). An initial axial stress of 0.5 MPa was applied on the specimen before hydration to ensure good contact and satisfactory load measurement (see Figure 6). When water injection

started, the piston was fixed and the build-up of axial stress was monitored by the load transducer.

2.2.3 Suction controlled oedometer test (SO-01 SO-04)

Controlled suction oedometer compression tests were carried out on samples of 10 mm in height and 38 mm in diameter by circulating vapour at controlled relative humidity at the base of the sample as shown in Figure 7 (tests SO-02/04). A high pressure oedometer frame was used so as to apply vertical stresses as high as 50 MPa (Marcial et al., 2002). Zero suction was applied by circulating pure water. Vertical strain was monitored using a digital micrometer (accuracy ± 0.001 mm).

Prior to compression, samples were hydrated under a low vertical stress of 0.1 MPa by applying a suction lower than the initial as-compacted value (estimated at 65 MPa from the water retention curve in Figure 8 at $w = 11\%$).

As seen in Table 4, the testing program includes 3 standard tests (SO-02 to 04) carried out on 38 mm diameter samples with an initial dry density of 1.67 Mg/m^3 under controlled suctions of 4.2, 12.6 and 38 MPa, respectively. Stabilisation of swelling under the imposed suctions and a vertical stress of 0.1 MPa were waited for prior to compression.

The configuration of test SO-01 ($\rho_{di} = 1.97 \text{ Mg/m}^3$, internal diameter of 35.13 mm), is similar to that described in Figure 6, with an annular void between the sample and ring corresponding to a 14% technological void. In this test, the sample was flooded with synthetic water, imposing zero suction through the liquid phase. The higher 1.97 Mg/m^3 density was chosen so as to correspond to the previous value of 1.67 Mg/m^3 once the technological void clogged by the lateral sample swelling. Obviously, even though that the global density of sample SO-01 was equal to that of samples SO-02/04 after swelling, the density of sample SO-01 should not be homogeneous and should follow a rather axisymetrical distribution, with lower values in the zone of former technological void clogged by soil swelling.

3 EXPERIMENTAL RESULTS

3.1 Water retention curves

Figure 8 presents the wetting path of the water retention curves (WRCs) obtained under both free swell and restrained swell conditions. For suctions higher than 9 MPa, the two curves are very similar while a significant difference can be identified in the range of suction below 9 MPa. When suction reached 0.01 MPa, the water content under free swell condition is 246.0%, a much higher value than that under restrained swell condition (25.4%). This confirms that the prevented swelling condition

significantly affects the retention property only in the range of low suctions (Yahia-Aissa et al. 2001, Cui et al. 2008, Ye et al. 2009).

The WRCs of samples of pure MX80 bentonite compacted to 1.7 Mg/m^3 dry unit mass under both free swell and constant volume conditions determined by Marcial (2003) are also presented in Figure 8. In the higher suction range ($s > 9 \text{ MPa}$), all data fall on the same curve, regardless of the imposed condition (swelling allowed or constant volume) and type and density of material (bentonite-sand mixture at 1.67 Mg/m^3 or pure bentonite at 1.7 Mg/m^3). By contrast, at lower suctions ($s < 9 \text{ MPa}$), the water content of the mixture under free swell condition is lower than that of the pure bentonite at the same suction value.

3.2 Effects of the technological void (tests SP01-SP04)

Figure 9 presents the results of the four tests (SP01-SP04) carried out to investigate the effect of technological void on the swelling pressure during water injection under a constant pressure of 0.1 MPa . As seen in Photo 1, some water escaping from the top of the cell was observed at the beginning of water injection during the initial increase of vertical stress (Figure 9). This phase of 25-30 min duration corresponded to the circulation of water in the annular gap between the sample and the ring. After this period, the gap was obviously filled by hydrated bentonite with no more outflow observed. After about 35 h, the vertical stress reached stabilization with final values of 2.07 , 2.77 , 2.44 , and 3.06 MPa for tests SP01 ($\rho_{di} = 1.93 \text{ Mg/m}^3$), SP02 ($\rho_{di} = 1.96 \text{ Mg/m}^3$), SP03 ($\rho_{di} = 1.96 \text{ Mg/m}^3$) and SP04 ($\rho_{di} = 1.98 \text{ Mg/m}^3$), respectively. Note that even though the piston was fixed (Figure 6), small volume changes (vertical displacements between 10 and $90 \mu\text{m}$) were recorded by the displacement transducer because of the deformability of the system.

3.3 Controlled suction compression tests (SO-01, SO-02, SO-03 and SO-04)

The changes in vertical strain with time during suction imposition for tests SO-01, SO-02, SO-03 and SO-04 are presented in Figure 10. In a standard fashion, higher vertical strain rates were observed at smaller suctions with final strains of 1.2% ($e = 0.69$), 5.4% ($e = 0.73$), 6.8% ($e = 0.75$) and 18.0% ($e = 0.97$) obtained for suctions of 38 MPa , 12.6 MPa , 4.2 MPa and 0 MPa , respectively.

The significantly faster hydration observed in test SO-01 (in which liquid water was used imposing a zero suction) was mainly due to the technological void that allowed water circulation around the sample. This first phase was comparable with that of tests SP-02/04 presented in Figure 9.

Figure 11 depicts the final void ratios obtained versus the imposed suctions in a semi-logarithmic plot. The points are reasonably located along a line and the following relationship can be derived:

$$e = -0.048 \ln(s) + 0.848 \quad (\text{Eq.1})$$

where e is the void ratio at equilibrium and s is suction in MPa.

Once equilibrated at the desired suction, samples were submitted to controlled-suction compression. The compression curves are presented in Figure 12 in a diagram giving the changes in void ratio e with respect to vertical net stress ($\sigma_v - u_a$) in which u_a is the air pressure, equal to the atmospheric pressure. Given the significant concerns about the validity of effective stress in unsaturated soils, it was preferred to use the independent variables approach involving the vertical net stress ($\sigma_v - u_a$) and suction ($s = u_w - u_a$), (Coleman 1962, Fredlund and Morgenstern, 1977, Gens 1996).

Initial void ratios were very different because of the significant dependence of initial swelling with respect to the suction imposed. Also, the sample SO-01 was not a homogeneous one, as commented above.

Each sample exhibited a slightly S-shaped compression curve. In a standard fashion, the compression curves are characterized by an initial linear branch with a low compressibility (pseudo-elastic domain) followed by a second branch with a higher compressibility (plastic domain) and a slight upward curvature at higher stresses.

As suggested by other authors (Keller et al., 2004; Tang et al., 2009), the points at high stresses were not used for determining the compression coefficient (C_c) and the yield stress (σ_y) delimitating the pseudo-elastic zone and the plastic one. Figure 13 shows the changes in yield stress with respect to suction. Also plotted in this Figure are the data obtained by Marcial (2003) on pure bentonite samples. Figure 13 confirms that suction decrease significant reduce the yield stress for both the mixture and pure bentonite samples. There is a linear relationship between yield stress and suction, and moreover, both curves are reasonably parallel. At a same suction, smaller yield stresses are observed for the mixture.

As also observed by Marcial (2003), the change in compression coefficient with respect to suction appeared to be non monotonic (Figure 14) with a decrease when suction was reduced from 38 MPa and 12.6 MPa, followed by an increase when suction was below 12.6 MPa. Comparison between pure bentonite and sand-bentonite mixture shows that at any suction, the latter appears to be more compressible with a larger compression coefficient.

3.4 Hydraulic conductivity measurements

The hydraulic conductivity of hydrated samples with initial technological void (tests SP2-SP4) was measured under constant head when applying the 0.1 MPa water pressure by recording the volume of injected water by means of a Pressure/Volume controller (no data were available for test SP01 due to a technical problem with the Pressure/Volume controller). The determination of hydraulic conductivity was done over the last 24 h once swelling stabilised. The hydraulic conductivity was also determined indirectly based on the consolidation curves during different compression stages of test SO-01 (see Figure 12) using Casagrande's method. As mentioned

before, the sample density was not homogeneous in those samples. Therefore, a non uniform hydraulic conductivity can be expected for each sample. The measured values correspond to the global hydraulic conductivity.

The changes in hydraulic conductivity with respect to dry density obtained from both methods are presented in Figure 15 and compared with constant head permeability measurements obtained by Gatabin et al. (2008) on homogeneous samples at similar densities. The data obtained for the heterogeneous samples with both methods are in good agreement. In a standard fashion, the hydraulic conductivity decreases with density increase following a slope comparable to that obtained by Gatabin et al. (2008). An in-depth examination shows that the samples tested here exhibit higher hydraulic conductivity than that by Gatabin et al. (2008), with a difference of one order of magnitude. This difference is suspected to be due to a preferential water flow in the looser zone (initial technological voids) around the samples.

4 INTERPRETATION AND DISCUSSION

In order to further analyse the effects of the technological void, various constitutive parameters of the compacted mixture are now defined (see Figure 16), such as for instance the bentonite void ratio (e_b). It is supposed that the volume of bentonite (V_b) in the mixture is equal to the difference between the total volume (V) and the volume of sand (V_s). V_b is equal to the sum of the bentonite particle volume (V_{bs}) and the volume of void, namely intra-void volume (V_i). The parameter e_b consists of two parts (Eq.2), the intra-bentonite void ratio inside the soil (e_{bi}) and the void ratio corresponding to the technological void (e_{tech}). Eq.3 and Eq. 4 define these two voids, respectively.

$$e_b = e_{bi} + e_{tech} \quad (\text{Eq.2})$$

$$e_{bi} = \frac{V_i}{V_{bs}} \quad (\text{Eq.3})$$

$$e_{tech} = \frac{V_{tech}}{V_{bs}} \quad (\text{Eq.4})$$

where V_{tech} is the volume of technological void. The value of e_{bi} can be deduced from the initial dry unit mass of the mixture (ρ_{dm}) using Eq.5 and Eq.6.

$$e_{bi} = \frac{G_{sb}\rho_w}{\rho_{db}} - 1 \quad (\text{Eq.5})$$

$$\rho_{db} = \frac{(B/100)\rho_m G_{ss}\rho_w}{G_{ss}\rho_w(1 + w_m/100) - \rho_m(1 - B/100)} \quad (\text{Eq.6})$$

where ρ_w is the water unit mass, G_{sb} is the specific gravity of bentonite, ρ_{db} is the

initial dry unit mass of bentonite in the mixture, which was calculated using Eq.6 (Dixon et al., 1985; Lee et al., 1999; Agus and Schanz, 2008; Wang et al., 2012), ρ_m is the unit mass of the mixture, B (%) is the bentonite content (in dry mass) in the mixture, G_{ss} is the specific gravity of sand, w_m is the water content of the mixture. In this study the decrease of water unit mass (ρ_w) during hydration (e.g. Skipper et al., 1991; Villar and Lloret, 2004) was not considered and the value was assumed to be constant (1.0 Mg/m^3), $B = 70\%$, $G_{ss} = 2.65$.

To analyse the water retention property under free swell condition, a parameter namely water volume ratio (e_w) defined as the ratio of water volume (V_w) to the bentonite volume (V_{bs}) is also adopted (Romero et al., 2011). This parameter can be deduced from the water content of the mixture (w_m) using the following equation:

$$e_w = \frac{w_m G_{sb}}{B} \quad (\text{Eq.7})$$

In the following, the two parameters e_b and e_w are used to analyze all experimental results obtained in order to evidence the effects of voids on the water retention capacity, the swelling pressure, the compressibility and the hydraulic conductivity.

4.1 Water retention curves

Figure 17a shows the changes in water volume ratio e_w of both the mixture and the pure bentonite with respect to suction under free swell condition. Unlike in the water content/suction plot (Figure 8), Figure 17a shows an excellent agreement with Marcial (2003)'s data on pure bentonite, with a unique relationship between e_w and suction along the wetting path with swelling. It confirms that water was only adsorbed in the bentonite (volume V_{bs}) and that the lower water content observed in the mixture at same suction (Figure 8) is related to the lower volume of bentonite in the mixture.

The results from the hydration tests on pure compacted bentonites under restrained swell condition with different void ratios (Marcial, 2003; Tang and Cui, 2010; Villar, 2005) are also presented in Figure 17. A phenomenon similar to that observed in the water content/suction plane (Figure 8) can be identified: in the range of low suctions ($<9 \text{ MPa}$ for the MX80 bentonite), the water retention property of bentonite depends strongly on the confining conditions; conversely, all curves become almost the same in the range of high suctions (as also observed by Agus 2005 and Agus et al. 2010) As suggested by Cui et al. (2002, 2008) and Ye et al. (2009), this confirms that the exfoliation of clay particles from the aggregates into inter-aggregate pores caused by hydration is moderate and can be accommodated at high suctions. By contrast, at lower suctions, available pores become completely full by hydrated clay particles and no more water can be adsorbed. This is not the case when swelling is allowed with much more water adsorbed. Figure 17b is a zoom of Figure 17a at small water volume ratios (between 0 and 1.5). The difference observed in the curves at constant volume

is due to differences in bentonite dry density ρ_{db} . When the full saturation is approached, samples with a higher bentonite void ratio (lower dry density) logically absorb more water for a given suction.

4.2 Hydration test with technological void

The values of vertical stress measured on heterogeneous samples at the end of the hydration tests on samples with technological voids (SP 01-04) are presented in Figure 18 with respect to the bentonite void ratio. Note that the bentonite void ratios for tests SP 01-04 were determined by taken into account the system deformation mentioned above (i.e. vertical displacements between 10 and 90 μm). The data of swelling stresses measured in homogeneous samples under the same conditions of constant volume by other authors are also plotted for comparison (MX80 70/30 bentonite/sand mixture from Karnland et al., 2008 and pure MX80 bentonite from Börgesson et al., 1996; Dixon et al., 1996; Karnland et al., 2008; Komine et al., 2009).

All data remarkably agree, providing a unique relationship between the vertical pressure and the bentonite void ratio, regardless of the sample nature (homogeneous or not). The correspondence with data from Karnland (pure bentonite and 70/30 bentonite sand mixture) at bentonite void ratio close to 1 is particularly good. The following expression can be deduced for the relationship between the axial stress (σ_s in MPa) and the bentonite void ratio e_b for the material studied here:

$$\sigma_s = 2.250e_b^{-1.149} \quad (\text{Eq.8})$$

This good correspondence between the response in swelling stress of homogeneous samples and that in axial stress of a hydrated heterogeneous sample indeed confirms that the stress at equilibrium is not affected by the heterogeneity of the samples. The pressure (σ_s in MPa) only depends on the global bentonite void ratio (e_b), regardless of the technological void and of the presence of sand.

In other words, during the hydration under constant global volume and in spite of their significant difference in form and dimension, the technological voids play the same role as the macro-pores of the homogeneous compacted bentonite in terms of filling voids by particle exfoliation, as commented above. The global final bentonite void ratio (or density) appears to be a relevant parameter allowing predicting the final axial stress obtained.

4.3 Compressibility

The interpretation of the compressibility data was based on the well known features of the aggregate microstructure of compacted soils that have been recalled above, showing in particular that the compression at constant water content of unsaturated compacted soils initially occurs by the collapse of large inter-aggregate pores full of air with little effect on the aggregates themselves. As a consequence, it was observed

that the changes in suction during compression at constant water content are negligible, since suction changes are governed by intra-aggregate clay water interactions that are little affected during compression (Li, 1995; Gens et al., 1995; Tarantino and De Col, 2008).

The compression curves of the homogeneous samples in Figure 12 (SP2 to 4) are further interpreted by an approximated estimation of the changes in degree of saturation during compression. This estimation is based on the assumption that the order of magnitude of the initial water contents of the samples hydrated from the initial as-compacted suction (65 MPa) at given suctions (38, 12.6 and 4.2 MPa) prior to compression can be obtained from the wetting path of the water retention curve in Figure 17. Based on this assumption, the water contents after hydration were determined, equal to 12.8, 16.8 and 18.6 % for suctions of 38, 12.6 and 4.2 MPa, respectively. The corresponding degrees of saturation are 52, 63 and 68%, respectively.

The application of suctions as high as 4.2, 12.6 and 38 MPa generated a moderate swelling of the samples, with void ratio increasing from the initial value of 0.64 to 0.75 at 4.2 MPa suction. In terms of microstructure, the changes corresponds to a moderate swelling of the aggregates within a structure still significantly desaturated with a maximum degrees of saturation of 68% at 4.2 MPa suction, indicating that the inter-aggregates pores remained full of air. During compression, the water content that was controlled within the aggregates did not suffer from any significant changes and the changes in degree of saturation could be estimated, as shown in Figure 19. The data show how the degree of saturation increase with increased stress and provide an estimation of the stress values at which saturation was reached (9, 14 and 27 MPa at $s = 4.2, 12.6$ and 38 MPa respectively). Once reported on the compression curves of Figure 12, we can observe that these stress values are located close to the inflection points observed on the curves, indicating that these points correspond to the saturation of the samples. In other words, the change in slope of the curves corresponds to the transition between two physical mechanisms, namely from the collapse of dry inter-aggregate pores to the expulsion of inter-aggregate adsorbed water. This is in agreement with the observation by Kochmanová and Tanaka (2011).

When the yield stress (σ_{v0}) in Figure 13 is plotted versus the corresponding bentonite void ratio (e_b) at the yield point (Figure 20), it appears that for both the mixture and pure bentonite, the yield stress increases sharply with decreasing bentonite void ratio. However, the curve of the mixture lies in the right of the pure bentonite's one, evidencing the role of sand in the compression behaviour. It can be concluded from Figure 20 that at the same bentonite void ratio, the mixture yields at a higher pre-consolidation stress.

4.4 Hydraulic conductivity

The values of global hydraulic conductivities presented in Figure 15 showed possible

preferential flow pathway in the case of heterogeneous samples with initial technological voids. This observation can be made also in Figure 21 in which the data of Figure 15 are re-plotted versus the bentonite void ratio and compared to other data of the pure MX80 bentonite (Karnland et al., 2008; Dixon et al., 1996) and of the 70/30 bentonite-sand mixture (Gatabin et al., 2008). The good agreement observed also confirms a negligible effect of sand on the hydraulic conductivity.

Note that the looser zone corresponding to the initial technological void is a weak zone with poorer mechanical resistance, at least on the short term. The question of the possible further changes that could occur on the long term is opened, given that some observations already showed that ageing effects are significant in compacted bentonite, both at microscopic scale (Delage et al. 2006) and macroscopic scale (Stroes-Gascoyne, 2010), showing a tendency towards density homogenisation. Further studies are needed to investigate the long term change in hydraulic conductivity of samples with initial technological voids.

5 CONCLUSION

The effects of voids on the hydro-mechanical properties of a compacted bentonite-sand mixture were studied. Water retention test, hydration test, suction controlled oedometer test and hydraulic test were performed on samples with different voids including the technological void and the void inside the soil. By introducing the parameters as bentonite void ratio and water volume ratio, the effects of voids on the water retention property, the swelling pressure, the compressibility and the hydraulic conductivity were analyzed.

Under different conditions (free swell and restrained swell), different water retention properties were observed depending on the suction value: at high suctions, the relation between the water volume ratio and the suction is unique, independent of the test conditions, indicating that the relatively limited exfoliated clay particles are mainly accommodated by the macro-pore of the soil. On the contrary, in the range of low suctions, the macro-pores available for accommodating exfoliated particles becomes limited in the case of restrained swell condition, explaining why less water is adsorbed in this case.

There is a unique relationship between the axial stress (for samples with technological void) or swelling pressure (constant volume condition) and the bentonite void ratio, regardless of the sample nature (homogeneous or not) and presence of sand, suggesting that the technological voids play the same role as the macro-pores of the homogeneous compacted bentonite. It also reveals that the swelling mechanisms of bentonite-sand mixture are the same as that of pure bentonite.

The change in slope of the compression curves corresponds to the transition between two physical mechanisms, namely from the collapse of dry inter-aggregate pores to

the expulsion of inter-aggregate adsorbed water.

At the same bentonite void ratio, bentonite/sand mixture yields at a higher pre-consolidation stress, evidencing the effect of sand on the compression behaviour.

Similar relationship between hydraulic conductivity and bentonite void ratio was observed for the bentonite-sand mixture and the pure bentonite without technological void; however, with the technological void in this study, the measured hydraulic conductivity for the same bentonite void ratio is generally higher, indicating the possible preferential flow pathway formed by the swollen soil that occupied the initial technological void.

From a practical point of view, the relationship elaborated between the hydro-mechanical behaviour with bentonite void ratio is helpful in designing the buffers/sealing elements with bentonite-based materials: if the bentonite proportion and the technological void are known, the specification of the buffer elements could be determined using the correlations elaborated in this study, according to the requirements in terms of swelling pressure and hydraulic conductivity. Then the water retention property and compressibility of the selected material can be evaluated. It should be however noted that the conclusion drawn here was based on the results of the bentonite/sand mixture with 70% of MX80 bentonite. Further experimental studies on other proportions and other bentonites are needed to generalise it.

ACKNOWLEDGEMENTS

The work was conducted in the framework of the SEALEX project of IRSN and the PHC Cai Yuanpei project (24077QE). The support of the National Nature Science Foundation of China (41030748) and that of the China Scholarship Council (CSC) are also greatly acknowledged.

REFERENCES

- AFNOR, 1992. AFNOR NF P94-057, Soils: investigation and testing. Granulometric analysis. Hydrometer method. Association Francaise de Normalisation. France.
- AFNOR, 1996. AFNOR NF P94-056, Soils: investigation and testing. Granulometric analysis. Dry sieving method after washing. Association Francaise de Normalisation. France.
- Agus, S.S, 2005. An Experimental study on hydro-mechanical characteristics of compacted bentonite-sand mixtures. PhD thesis. Weimar.
- Agus, S.S., and Schanz, T., 2008. A method for predicting swelling pressure of compacted bentonites. *Acta Geotechnica*, 3(2), 125-137.
- Agus, S.S., and Schanz, T., and Fredlund, D.G., 2010. Measurements of suction versus water content for bentonite-sand mixtures. *Can. Geotech. J.*, 47, 583-594.
- Ahmed. S., Lovell. C.W. & Diamond. S. 1974. Pore sizes and strength of compacted clay. *ASCE Journal of the Geotechnical Engineering Division* 100, 407-425.

557 Andra, 2005. Référentiel des matériaux d'un stockage de déchets à haute activité et à vie
 558 longue - Tome 4: Les matériaux à base d'argilites excavées et remaniées. Rapport Andra
 559 N° CRPASC040015B.
 560 Barnichon, J.D. and Deleruyelle, F., 2009. Sealing Experiments at the Tournemire URL.
 561 EUROSAFE.
 562 Börgesson, L., Karnland, O., Johannesson L.E., 1996. Modelling of the physical behaviour of
 563 clay barriers close to water saturation.pdf: Modelling of the physical behaviour of clay
 564 barriers close to water saturation.Engineering Geology 41, 127-144.
 565 Coleman, J.D. 1962. Stress-Strain relations for partially saturated soils. Géotechnique 12 (4),
 566 348-350.
 567 Cui, Y.J., Loiseau, C. and Delage, P., 2002. Microstructure changes of a confined swelling soil
 568 due to suction controlled hydration. Unsaturated soils: proceedings of the Third
 569 International Conference on Unsaturated Soils, 10-13, March 2002, Recife, Brazil,
 570 593-598.
 571 Cui, Y.J., Tang, A.M., Loiseau, C., Delage, P., 2008. Determining the unsaturated hydraulic
 572 conductivity of a compacted sand-bentonite mixture under constant-volume and
 573 free-swell conditions. Physics and Chemistry of the Earth, Parts A/B/C, 33 (Supplement
 574 1), S462 - S471.
 575 Cui, Y.J., Tang, A.M., Qian, L.X., Ye, W.M., Chen, B., 2011. Thermal-mechanical behavior of
 576 compacted GMZ Bentonite. Soils and Foundations, Vol. 51, No. 6, 1065-1074.
 577 Delage P. & Graham J. 1995. The mechanical behaviour of unsaturated soils. Proceedings of
 578 the 1st International Conference on Unsaturated soils, Vol. 3, 1223-1256, Paris, E.E.
 579 Alonso and P. Delage eds, Balkema.
 580 Delage, P., Audiguier, M., Cui, Y.J. & Howat, M.D. 1996. Microstructure of a compacted silt.
 581 Canadian Geotechnical Journal, 33 (1), 150-158.
 582 Delage, P., Howat, M.D., Cui, Y.J., 1998. The relationship between suction and swelling
 583 properties in a heavily compacted unsaturated clay. Engineering Geology, 50(1-2),
 584 31-48.
 585 Delage, P., Marcial, D., Cui, Y.J., Ruiz, X., 2006. Ageing effects in a compacted bentonite: a
 586 microstructure approach. Géotechnique 56 (5), 291-304.
 587 Delage, P. and Cui, Y.J. 2008a. An evaluation of the osmotic method of controlling suction.
 588 Journal of Geomechanics and Geoengineering 3 (1), 1-11.
 589 Delage, P. and Cui, Y.J. 2008b. A novel filtration system for polyethylene glycol solutions
 590 used in the osmotic method of controlling suction. Canadian Geotechnical Journal 45,
 591 421-424.
 592 Dixon, D.A., Gray, M.N. and Thomas, A.W., 1985. A study of the compaction properties of
 593 potential clay-sand buffer mixtures for use in nuclear fuel waste disposal. Engineering
 594 Geology, 21, 247-255.
 595 Dixon, D.A., Gray, M.N., Hnatiw, D., 1992. Critical gradients and pressures in dense swelling
 596 clays. Canadian Geotechnical Journal 29 (6), 1113-1119.
 597 Dixon, D.A., Gray, M.N., Graham, J., 1996. Swelling and hydraulic properties of bentonites
 598 from Japan, Canada and USA. In Proceedings of the second International Congress on
 599 Environmental Geotechnics, Osaka, Japan, 5-8.
 600 Fredlund D.G. & Morgenstern N.R. 1977. Stress state variables for unsaturated soils. ASCE J.

Geotech. Eng. Div. GT5, 103, 447-466.

Gatabin, C., Touze, G., Imbert, C., Guillot, W., Billaud, P., 2008. ESDRED Project, Module 1-Selection and THM characterization of the buffer material. In International conference underground disposal unit design&emplacement processes for a deep geological repository, 16-18 June, Prague.

Gens, A., Alonso, E.E., Suriol, J., Lloret, A., 1995. Effect of structure on the volumetric behaviour of a compacted soil. In: Alonso, Delage (Eds.), Proc. 1st Int. Conf. on Unsaturated Soils, Paris, vol. 1. Balkema, Rotterdam, 83-88.

Gens, A., 1996. Constitutive modelling : Application to compacted soils . Proc. 1st Int. Conf on Unsaturated Soils UNSAT' 95, Vol. 3, 1179-1200, Paris.

Juvankoski, M., 2010. Description of basic design for buffer (working report 2009-131). Technical report, EURAJOKI , FINLAND.

Karnland, O., Nilsson, U., Weber, H., and Wersin, P., 2008. Sealing ability of Wyoming bentonite pellets foreseen as buffer material-Laboratory results. Physics and Chemistry of the Earth, Parts A/B/C, 33, S472-S475.

Keller, T., Arvidsson, J., Dawidowski, J.B., Koolen, A.J., 2004. Soil precompression stress. II. A comparison of different compaction tests and stress - displacement behaviour of the soil during wheeling. Soil Till. Res. 77, 97-108.

Kochmanová, N., Tanaka, H., 2011. Influence of the Soil Fabric on the Mechanical Behaviour of Unsaturated and Saturated Clay. Soils and Foundations, Vol. 51, No. 2, 275-286.

Komine, H. and Yasuhara, K. and Murakami, S. 2009. Swelling characteristics of bentonites in artificial seawater. Canadian Geotechnical Journal. 46, 177-189

Komine, H., 2010. Predicting hydraulic conductivity of sand bentonite mixture backfill before and after swelling deformation for underground disposal of radioactive wastes. Engineering Geology. 114, 123-134

Komine, H., Watanabe, Y., 2010. The past, present and future of the geo-environment in Japan. Soils and Foundations, Vol. 50 (2010) No. 6 977-982.

Lee, J.O., Cho, W.J. and Chun, K.S., 1999. Swelling Pressures of a Potential Buffer Material for High-Level Waste Repository. Journal of the Korean Nuclear Society, 31, 139-150.

Li, Z.M., 1995. Compressibility and collapsibility of compacted unsaturated loessial soils. In: Alonso, Delage (Eds.), Proc. 1st Int. Conf. on Unsaturated Soils, Paris, vol. 1. Balkema, Rotterdam, 139-144.

Lloret, A., Villar, M., 2007. Advances on the knowledge of the thermo-hydro-mechanical behaviour of heavily compacted FEBEX bentonite. Physics and Chemistry of the Earth, 32, 701-715

Marcial, D., Delage, P. and Cui, Y.J. 2002. On the high stress compression of bentonites. Canadian Geotechnical Journal 39, 812-820.

Marcial, D., 2003. Comportement hydromécanique et microstructural des matériaux de barrière ouvragée, thèse ENPC.

Martin, P.L., Barcala, J.M., and Huertas, F., 2006. Large-scale and long-term coupled thermo-hydro-mechanic experiments with bentonite: the febex mock-up test. Journal of Iberian Geology, 32(2), 259-282.

Montes-H, G., Duplay, J., Martinez, L., and Mendoza, C. 2003. Swelling–shrinkage kinetics of MX80 bentonite. Applied Clay Science, 22, 279-293.

- Pusch, R., 1979, Highly compacted sodium bentonite for isolating rock-deposited radioactive waste products. Nucl. Technol.:(United States), 45(2).
- Romero, E., Gens, A. & Lloret, A., 1999. Water permeability, water retention and microstructure of unsaturated compacted Boom clay. Engineering Geology. 54, 117-127.
- Romero, E., Della Vecchia, G., and Jommi, C., 2011. An insight into the water retention properties of compacted clayey soils. Geotechnique 61, No. 4, 313-328.
- Skipper, N.T., Refson, K., McConnell, J.D.C., 1991. Computer simulation of interlayer water in 2:1 clays. J. Chem. Phys. 94 (11), 7434-7445.
- Sridharan, A., Altschaeffle, A. G. and Diamond, S. (1971), Pore size distribution studies, Journal of the Soil Mechanics and Foundations Division, Proceedings of the ASCE, vol. 97, SM 5, 771-787
- Stroes-Gascoyne, S. 2010. Microbial occurrence in bentonite-based buffer, backfill and sealing materials from large-scale experiments at AECL's underground research laboratory. Applied Clay Science, 47(1-2), 36-42.
- Tang, A.M., Cui, Y.J., Eslami, J. Defossez, P., 2009. Analysing the form of the confined uniaxial compression curve of various soils . Geoderma vol (148)3-4, 282-290.
- Tang, A.M and Cui, Y.J., 2010, Effects of mineralogy on thermo-hydro-mechanical parameters of MX80 bentonite, Journal of Rock Mechanics and Geotechnical Engineering. 2 (1), 91-96.
- Tarantino, S. and De Col, E., 2008. Compaction behaviour of clay. Géotechnique, vol. 58 (3), 199-213.
- Villar, M.V. and Lloret. A., 2004. Influence of temperature on the hydro-mechanical behaviour of a compacted bentonite. Applied Clay Science, 26(1-4), 337-350.
- Villar, M.V., 2005, MX-80 Bentonite. Thermo-Hydro-Mechanical Characterisation Performed at CIEMAT in the Context of the Prototype Project. CIEMAT Technical Report: CIEMAT/DIAE/54540/2/04.
- Villar, M.V., Lloret, A., 2008. Influence of dry density and water content on the swelling of a compacted bentonite. Applied Clay Science, 39(1-2), 38-49.
- Wang Q., Tang A.M., Cui Y.J., Delage P., Gatmiri B. 2012. Experimental study on the swelling behaviour of bentonite/claystone mixture. Engineering Geology 124, 59-66.
- Yahia-Aissa, M., Delage, P., & Cui, Y.J. 2001. Suction-water relationship in swelling clays. Clay science for engineering, IS-Shizuoka International Symposium on Suction, Swelling, Permeability and Structure of Clays, 65-68, Adachi & Fukue eds, Balkema.
- Ye, W.M., Cui, Y.J., Qian, L.X., and Chen. B., 2009. An experimental study of the water transfer through confined compacted gmz bentonite. Engineering Geology, 108(3-4), 169-176.
- Yong, R.N., Boonsinsuk, P., and Wong, G., 1986. Formulation of backfill material for a nuclear fuel waste disposal vault. Canadian Geotechnical Journal, 23(2), 216-228.

List of Tables

689	Table 1 Chemical composition of the synthetic water
690	Table 2 Test conditions for water retention property
691	Table 3 Specimens used for swelling pressure test
692	Table 4 Specimens used for suction controlled oedometer test

694 **List of Figures**

696	Figure 1. Grain size distribution of the MX80 bentonite and sand
697	Figure 2. X-Ray curves of the MX80 bentonite
698	Figure 3. Hermetic plastic container with a vapor circulation system for adjusting water
699	content
700	Figure 4. Pore size distribution of bentonite/sand mixture compacted to different dry density
701	with a water content of about 11.0%
702	Figure 5. Constant volume cell for WRC determination. (a) Osmotic method; (b) Vapour
703	equilibrium technique
704	Figure 6. Schematic layout of hydration test with technological void
705	Figure 7. Experimental setup of suction controlled oedometer test
706	Figure 8. WRCs of bentonite-sand mixture and pure bentonite
707	Figure 9. Evolution of the axial stress for all hydration tests with technological void
708	Figure 10. Evolution of vertical strain during suction imposition
709	Figure 11. Relationship between void ratio and suction for the compacted sand bentonite
710	mixture
711	Figure 12. Void ratio of soil versus vertical net stress for different suctions
712	Figure 13. Changes in yield stress with suction
713	Figure 14. Changes in compression coefficient with suction
714	Figure 15. Hydraulic conductivity versus dry density of mixture
715	Figure 16. Composition of the bentonite/sand mixture
716	Figure 17. Water volume ratio (e_w) Versus suction. a) full range of water volume ratio; b) zoom
717	on the range of low water volume ratio
718	Figure 18. Relationship between vertical stress or axial stress and bentonite void ratio
719	Figure 19. Changes in degree of saturation during compression
720	Figure 20. Relationship between yield stress and bentonite void ratio
721	Figure 21. Hydraulic conductivity versus bentonite void ratio

723 **List of Photos**

725	Photo 1. Water outflow through the technological void.
-----	--

Table 1. Chemical composition of the synthetic water

Components	NaHCO ₃	Na ₂ SO ₄	NaCl	KCl	CaCl ₂ .2H ₂ O	MgCl ₂ .6H ₂ O	SrCl ₂ .6H ₂ O
Mass (g) per Litter of solution	0.28	2.216	0.615	0.075	1.082	1.356	0.053

Table 2. Test conditions for water retention property

Suction control method	Suction (MPa)	constant volume	Free swell
LiCl	309	—	√
K ₂ CO ₃	113	—	√
Mg(NO ₃) ₂	82	—	√
Saturated NaCl	38	√	√
salt solution (NH ₄) ₂ SO ₄	24.9	√	√
ZnSO ₄	12.6	√	√
KNO ₃	9.0	√	√
K ₂ SO ₄	4.2	√	√
Concentration of PEG solution (g PEG/g Water)	0.302	1	√
	0.095	0.1	√
	0.030	0.01	√

Table 3. Specimens used for swelling pressure test

Tests	Compaction Stress (MPa)	Compacted dry density (Mg/m ³)
SP01	65	1.93
SP02	70	1.96
SP03	80	1.96
SP04	85	1.98

Table 4 Specimens used for suction controlled oedometer test

Tests	ρ _{di} (Mg/m ³)	D (mm)	s (MPa)
SO-01	1.97	35.13	0
SO-02	1.67	38.00	4.2
SO-03	1.67	38.00	12.6
SO-04	1.67	38.00	38

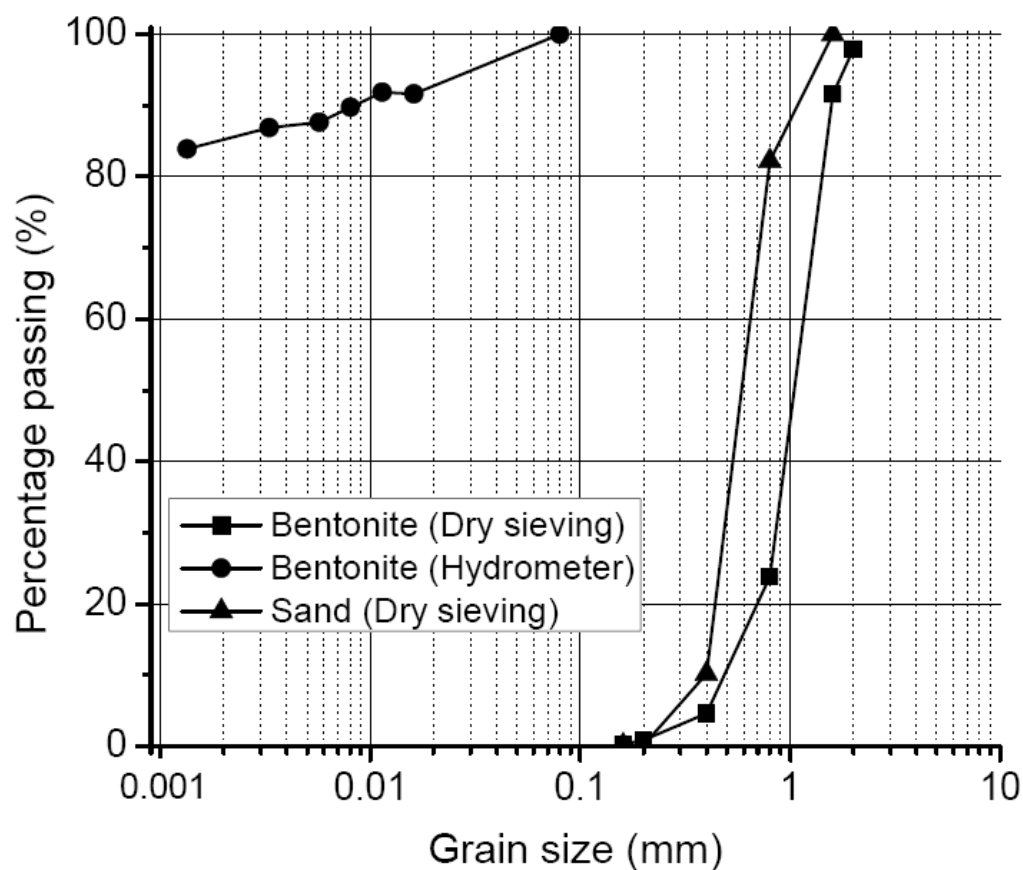


Figure 1. Grain size distribution of the MX80 bentonite and sand

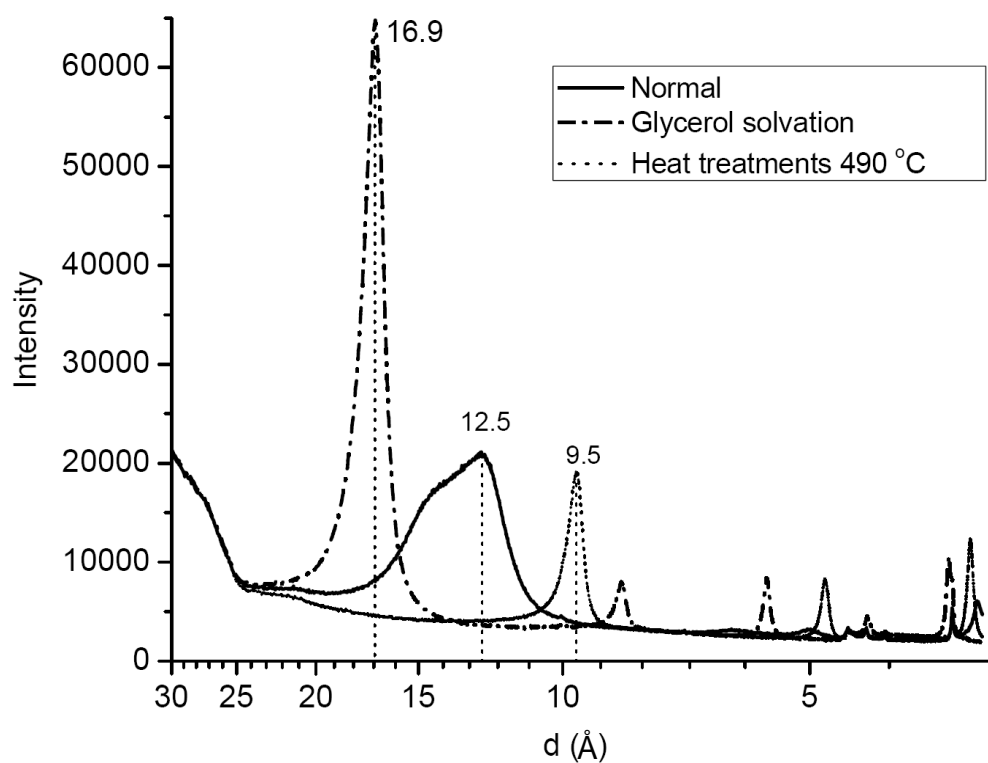


Figure 2. X-Ray curves of the MX80 bentonite

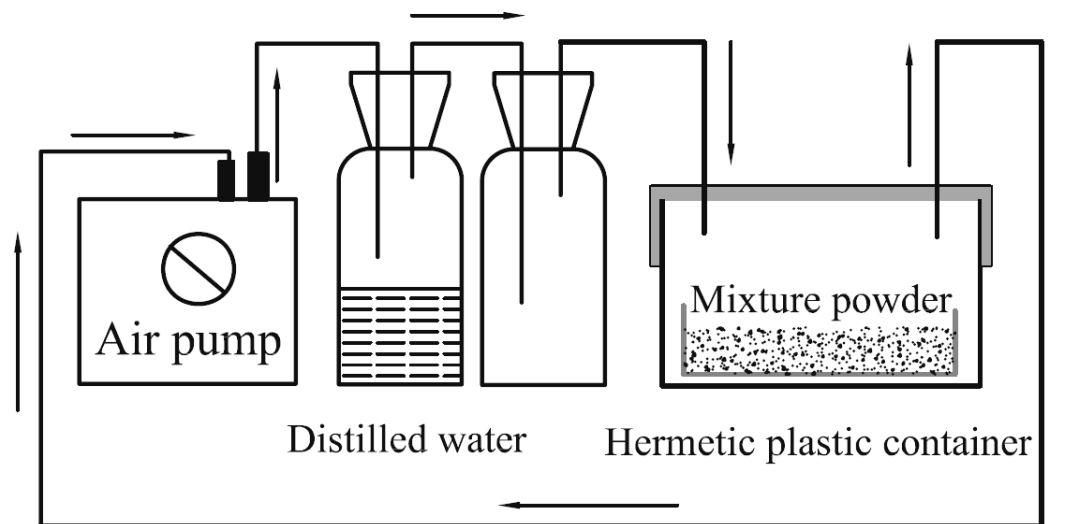


Figure 3. Hermetic plastic container with a vapor circulation system for adjusting water content

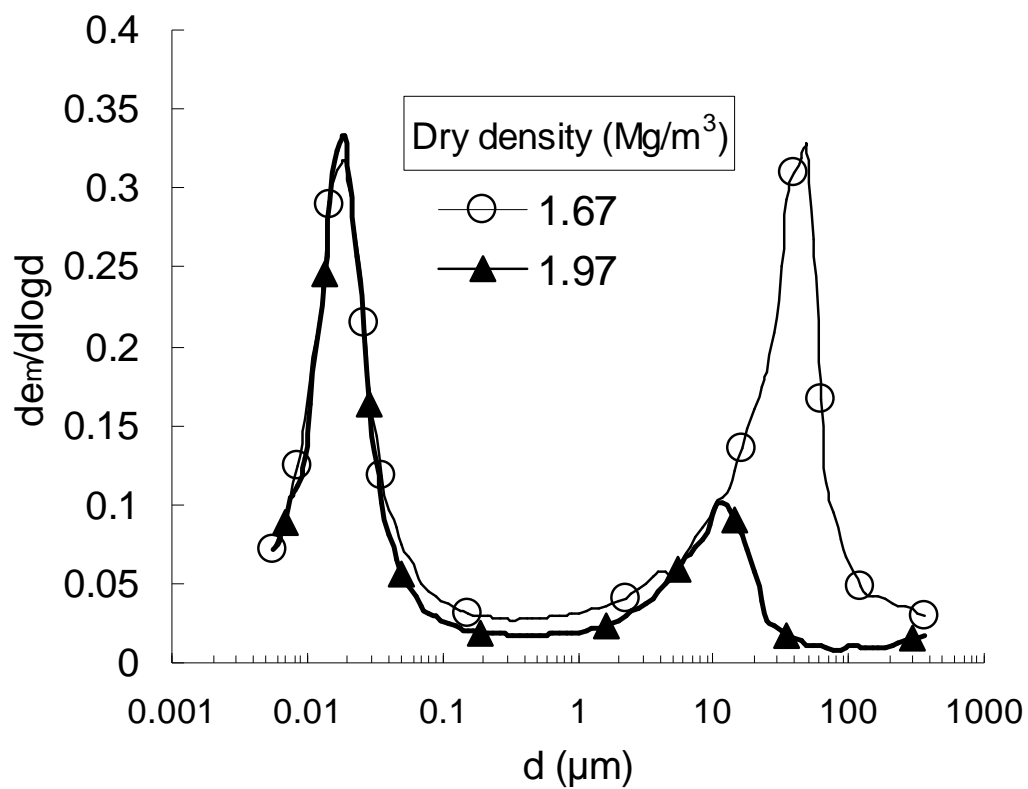
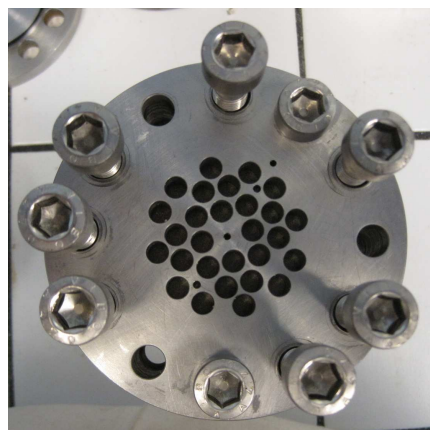
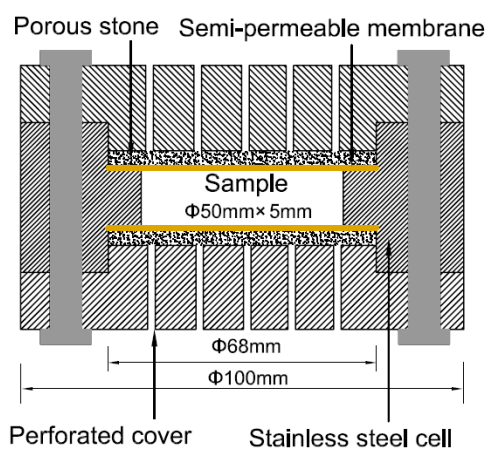
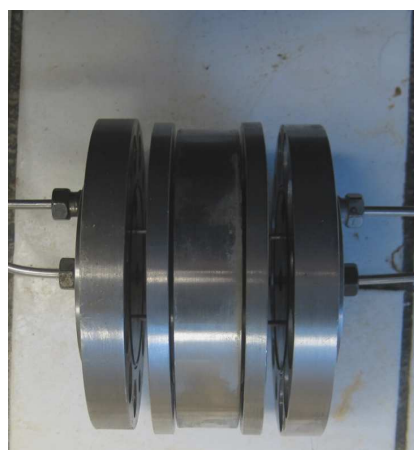
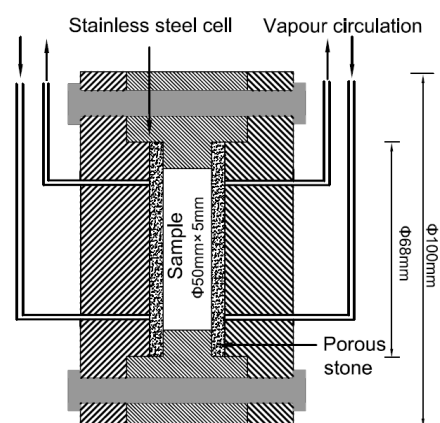


Figure 4. Pore size distribution of bentonite/sand mixture compacted to different dry density with a water content of about 11.0%



(a)



(b)

Figure 5. Constant volume cell for WRC determination. (a) Osmotic method; (b) Vapour equilibrium technique

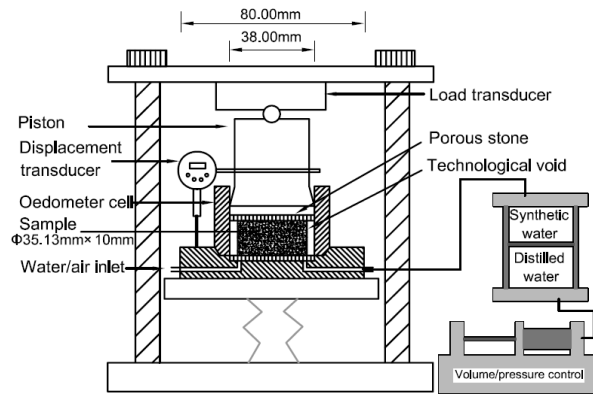


Figure 6. Schematic layout of hydration test with technological void

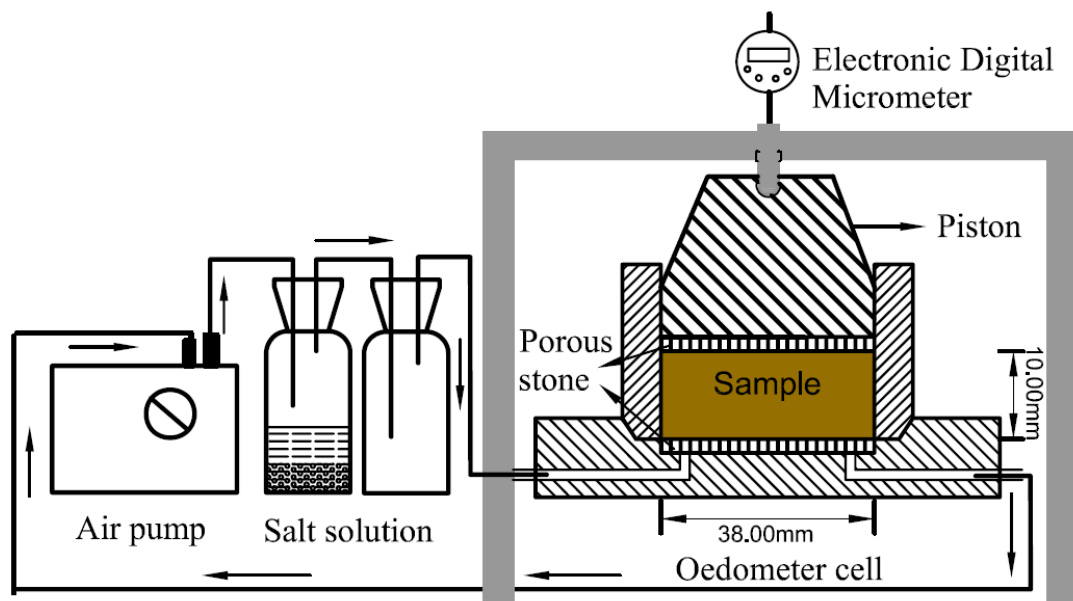


Figure 7. Experimental setup of suction controlled oedometer test

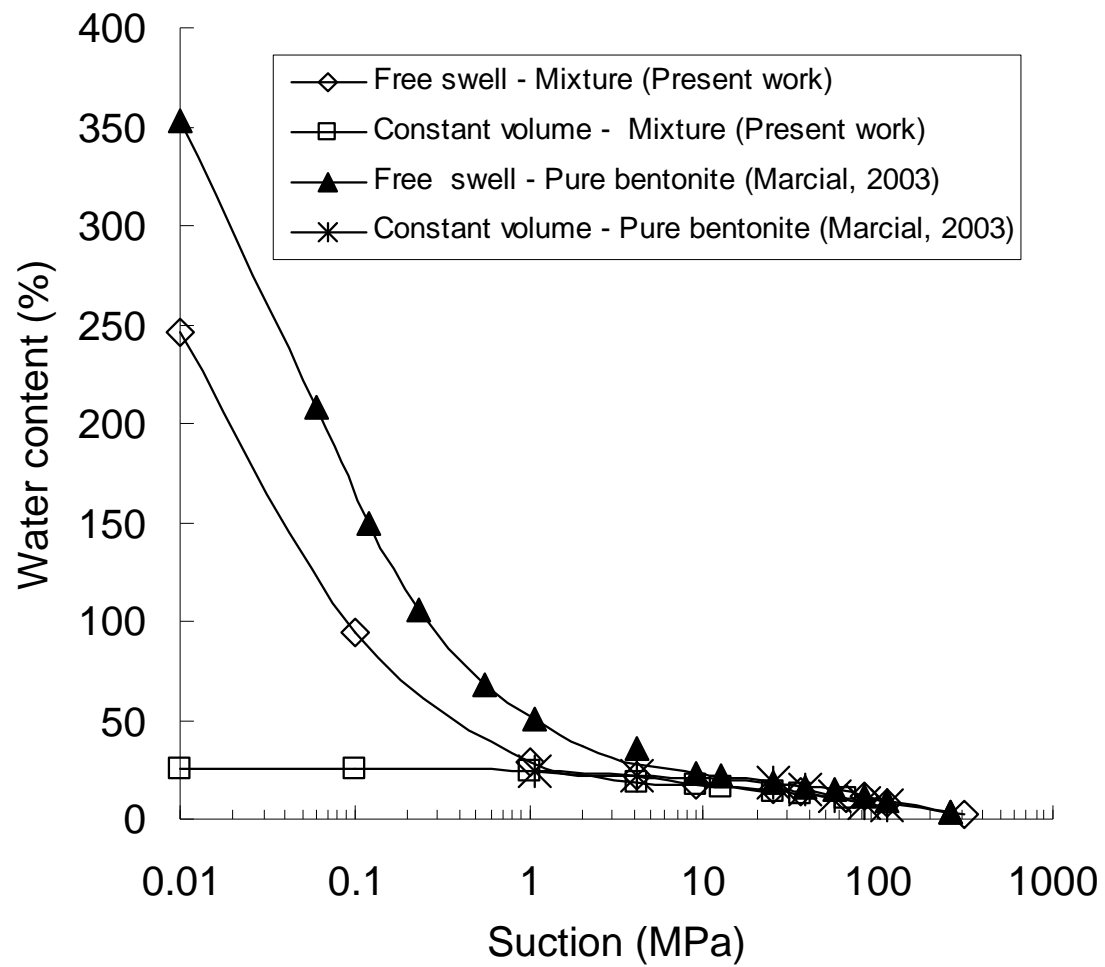


Figure 8. WRCs of bentonite-sand mixture and pure bentonite

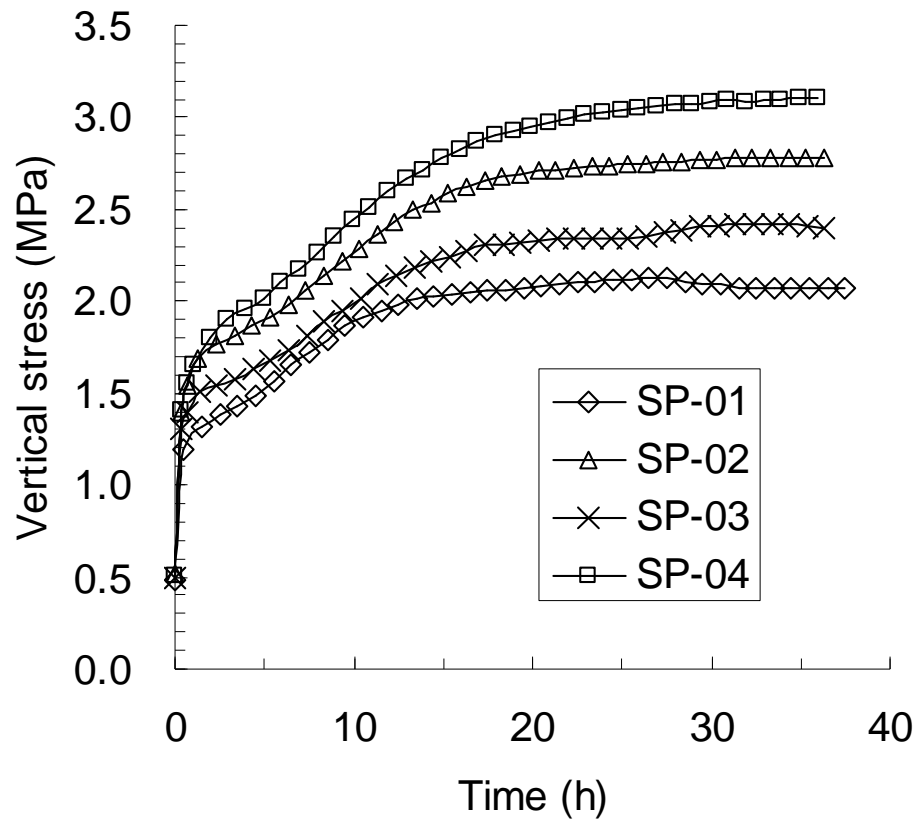


Figure 9. Evolution of the vertical stress for all hydration tests with technological void

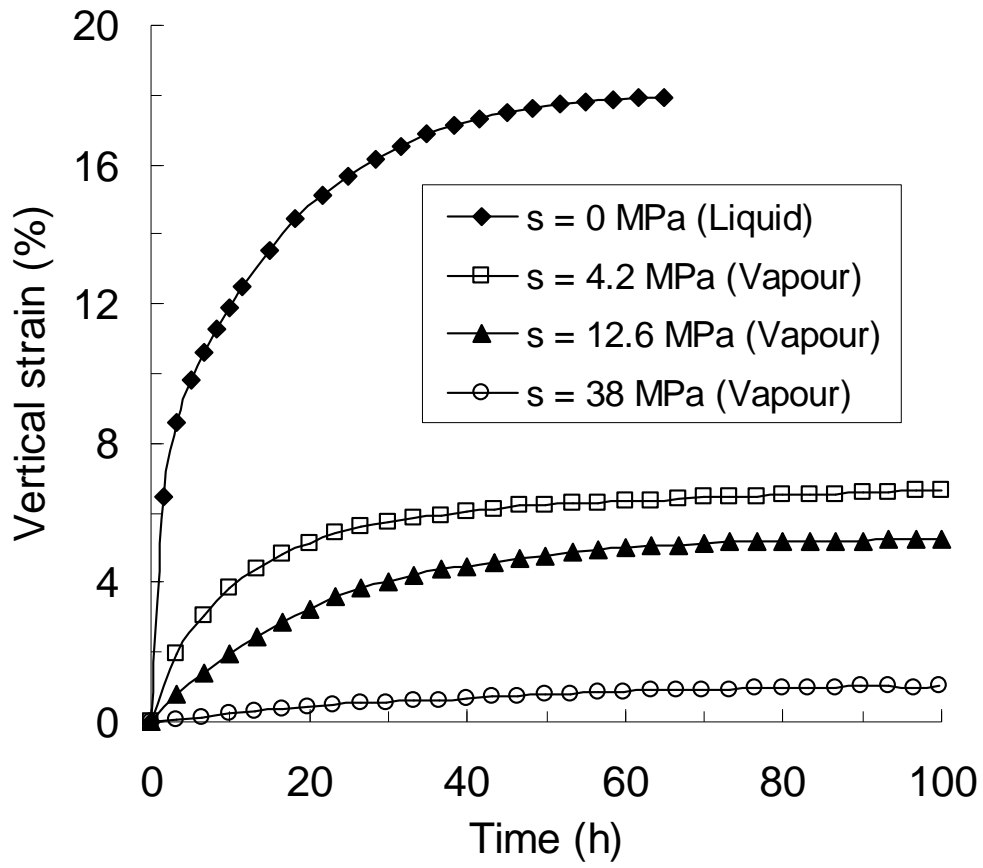


Figure 10. Evolution of vertical strain during suction imposition

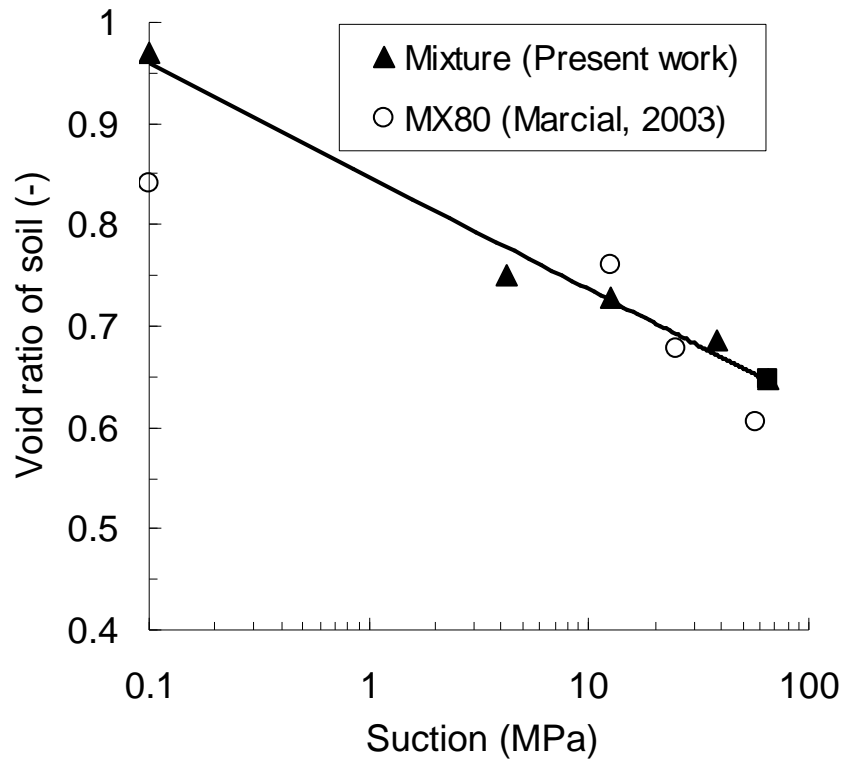


Figure 11. Relationship between void ratio and suction for the compacted sand bentonite mixture.

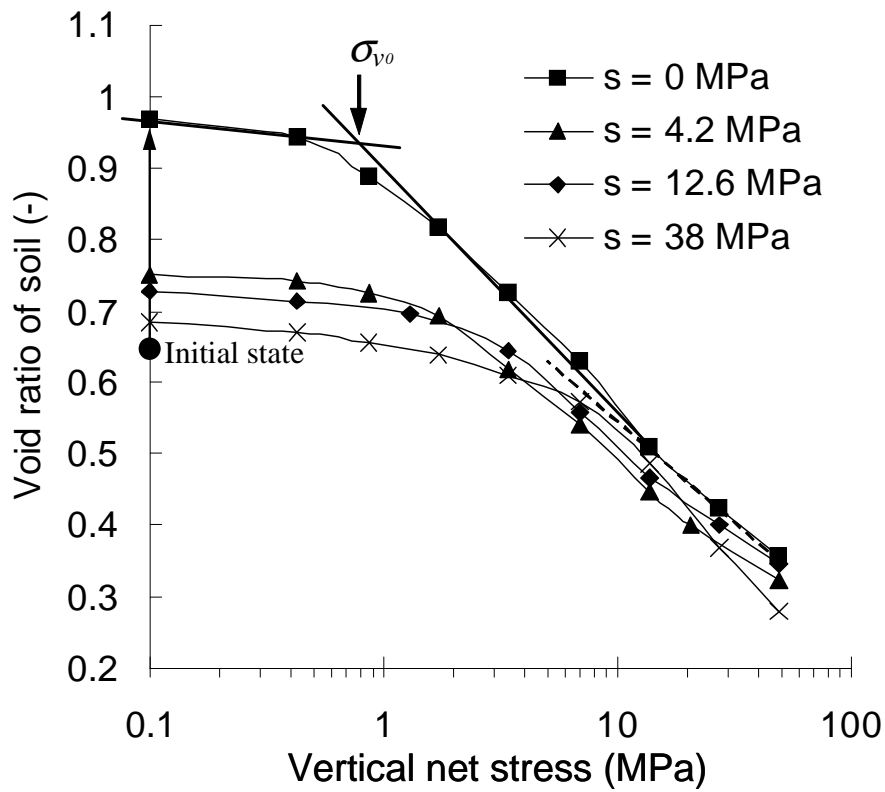


Figure 12. Void ratio of soil versus vertical net stress for different suctions

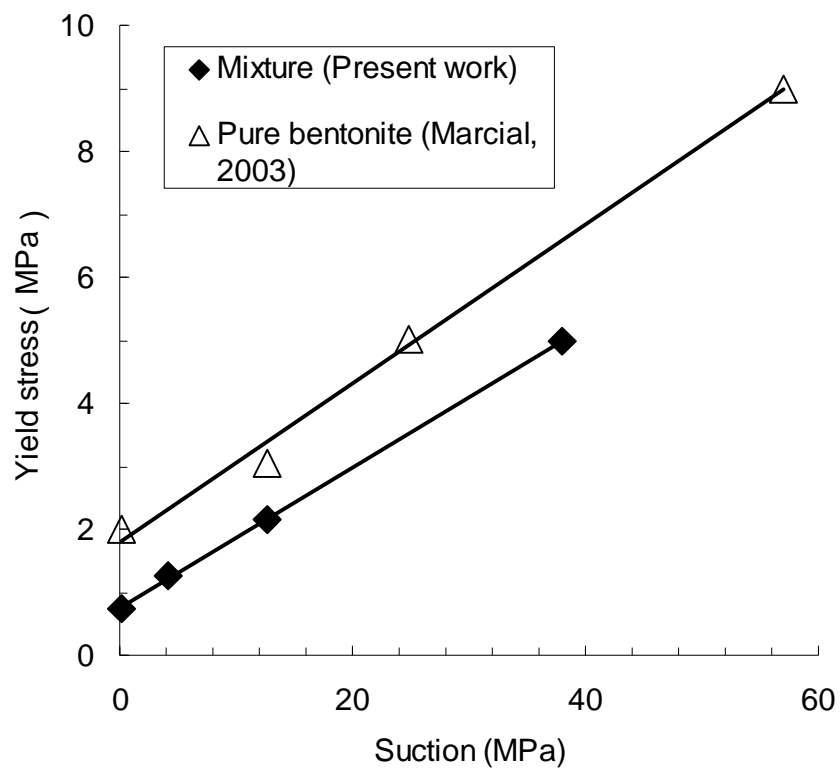
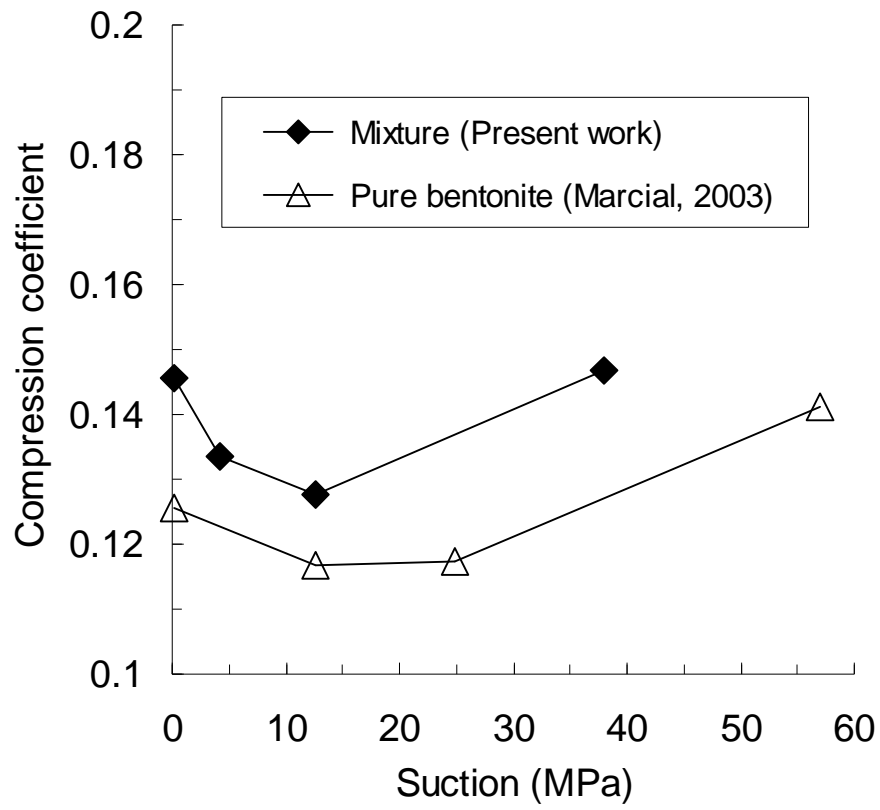


Figure 13. Changes in yield stress with suction



830

831 Figure 14. Changes in compression coefficient with suction

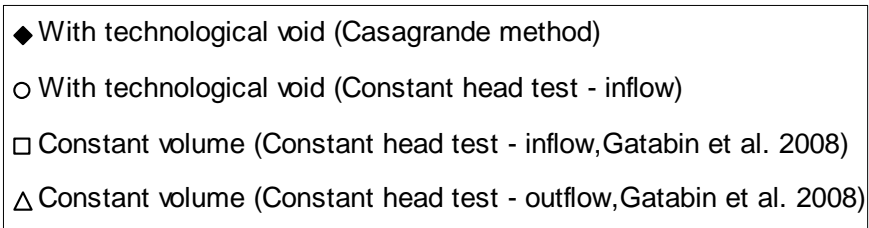
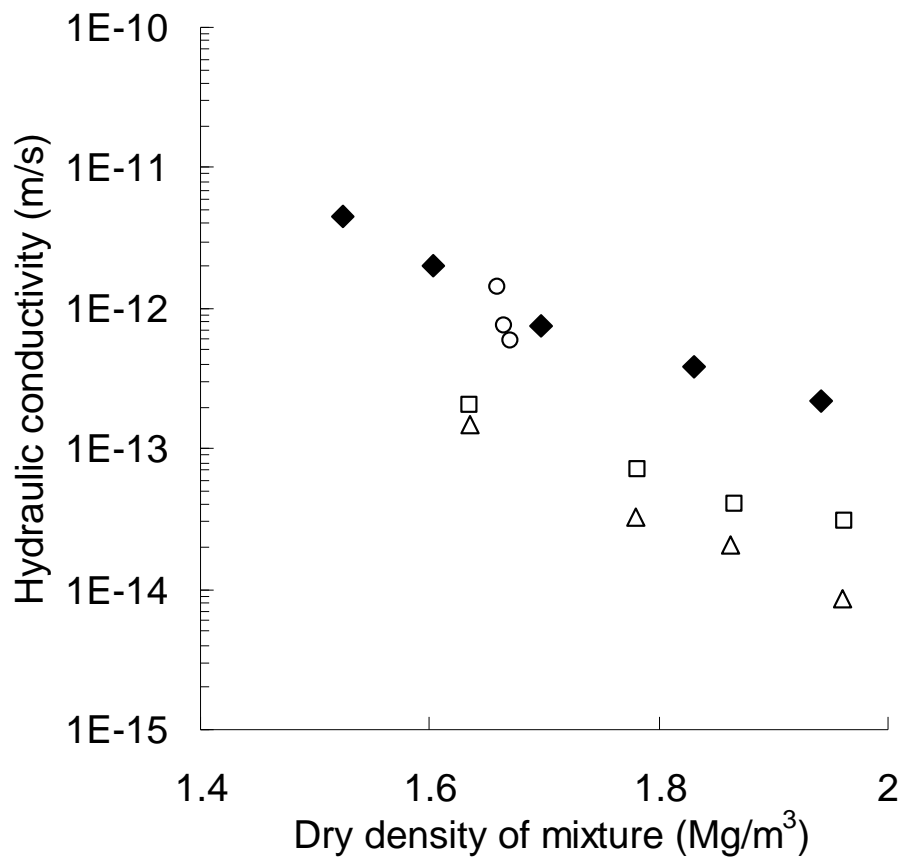


Figure 15. Hydraulic conductivity versus dry density of mixture

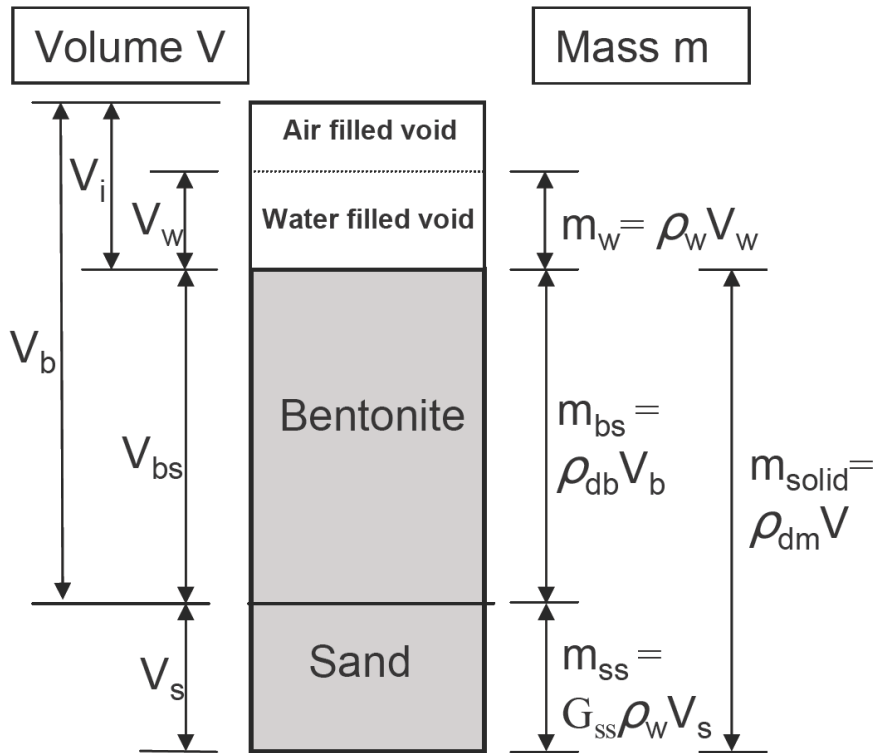
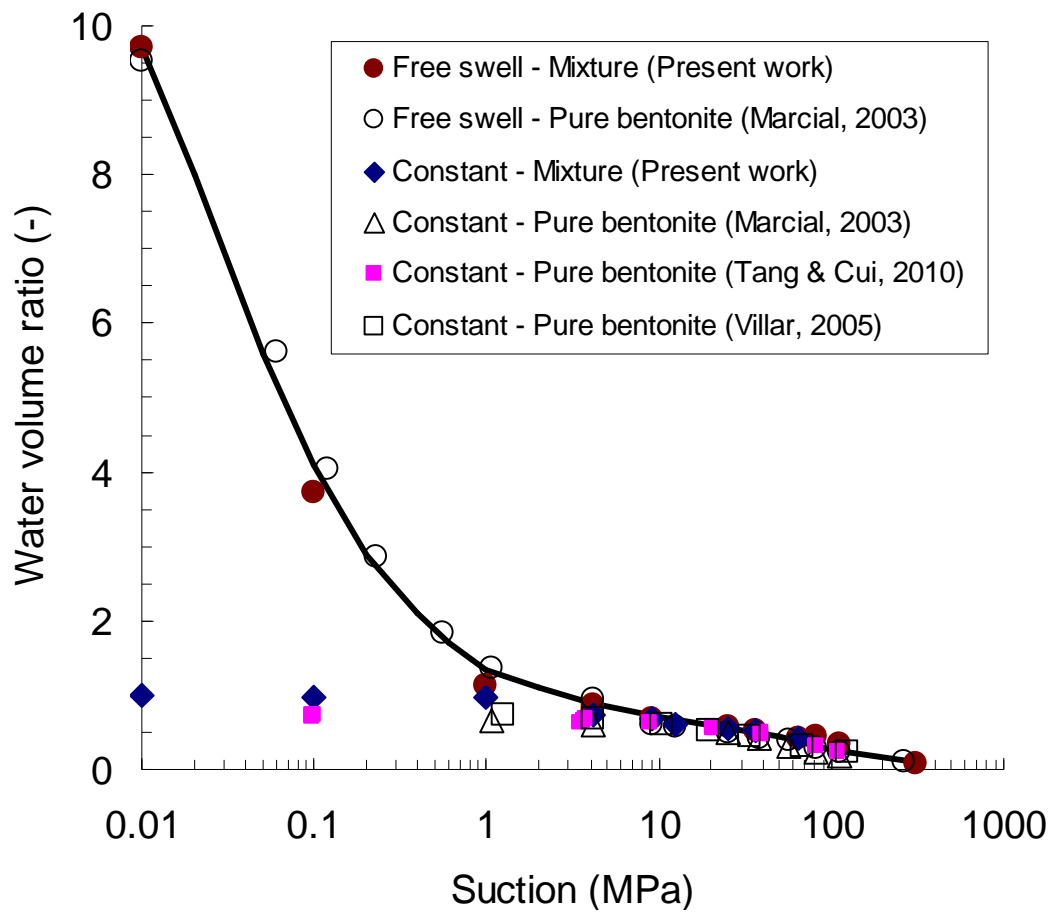
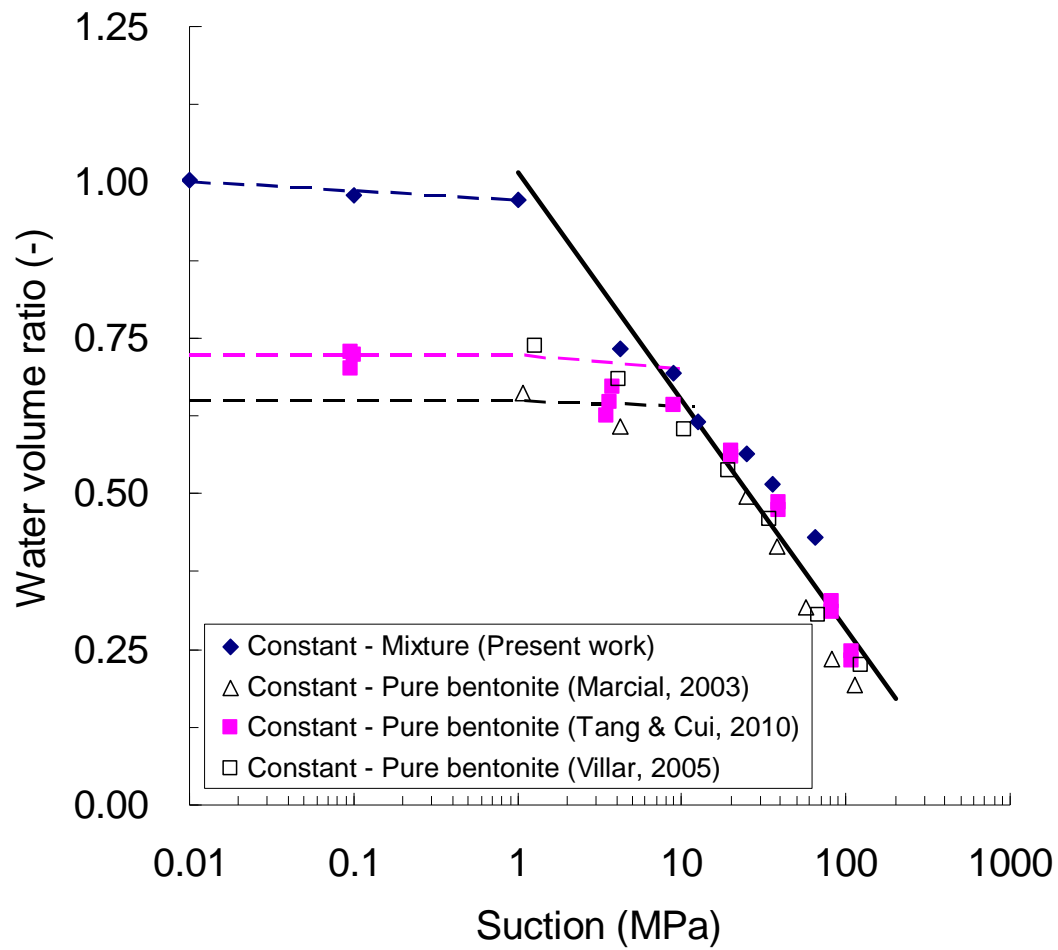


Figure 16. Composition of the bentonite/sand mixture



(a)



$\rho_{db} = 1.70 \text{ Mg/m}^3$ (Marcial, 2003);
 $\rho_{db} = 1.60 \text{ Mg/m}^3$ (Tang et al., 2010; Villar, 2005);
 $\rho_{db} = 1.43 \text{ Mg/m}^3$ (Present work);

b)

Figure 17. Water volume ratio (e_w) Versus suction. a) full range of water volume ratio; b) zoom on the range of low water volume ratio

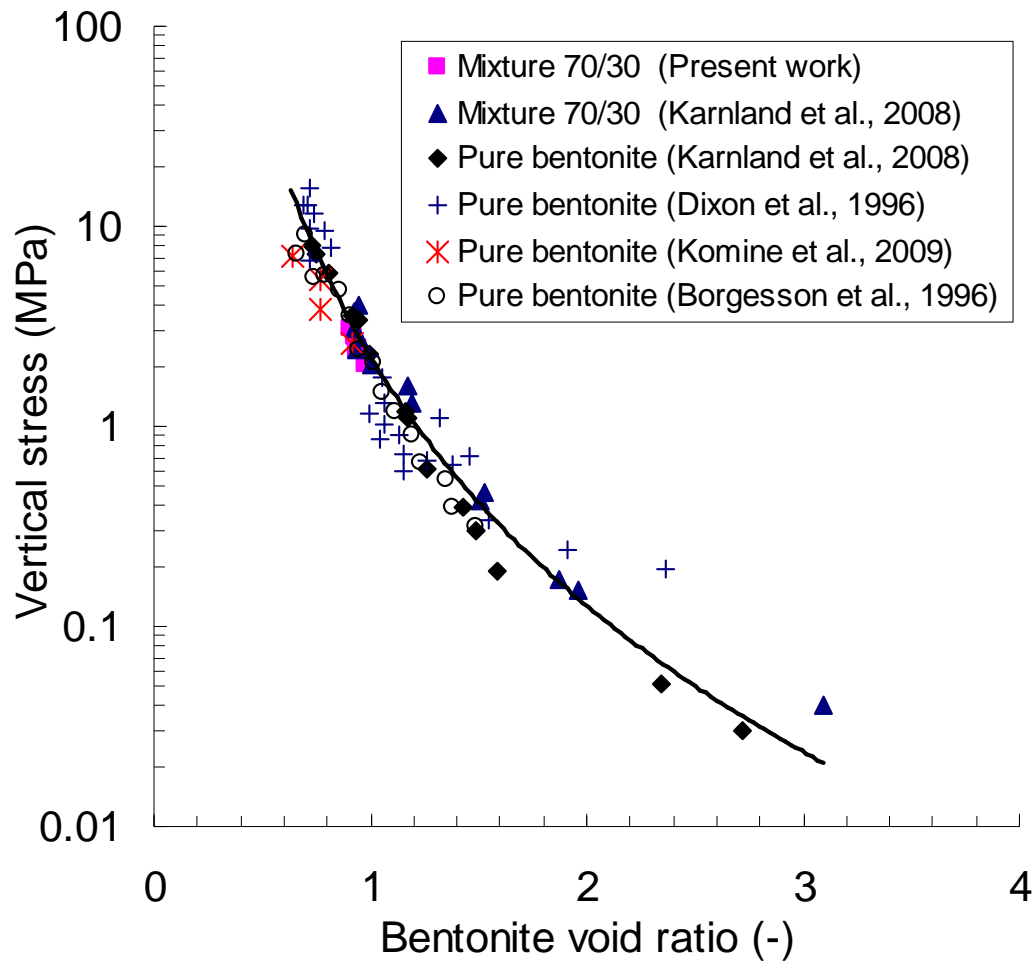


Figure 18. Relationship between vertical stress and bentonite (MX 80) void ratio

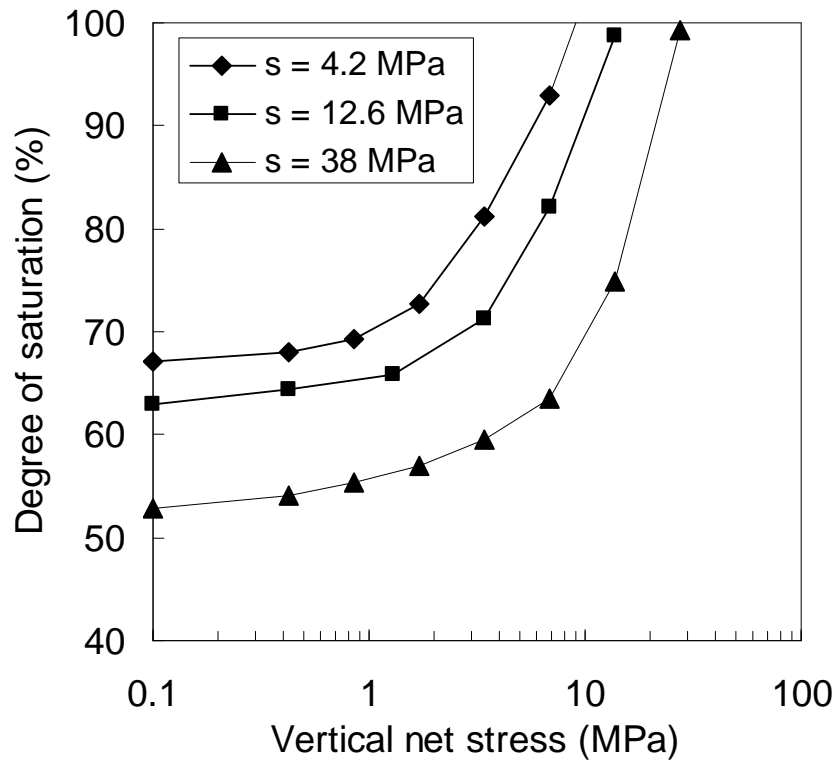


Figure 19. Changes in degree of saturation during compression

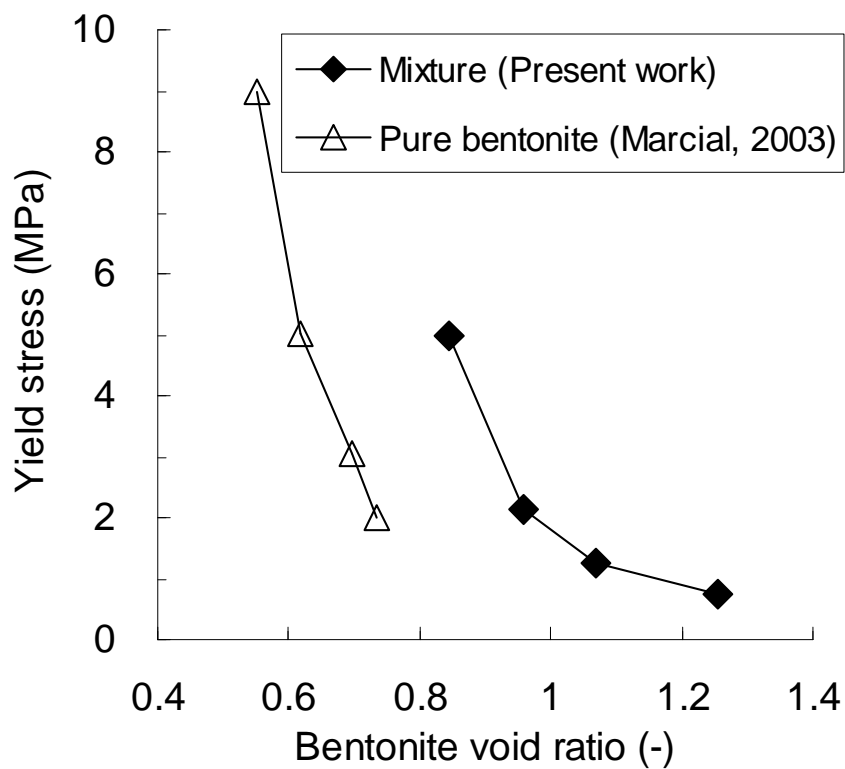


Figure 20. Relationship between yield stress and bentonite void ratio

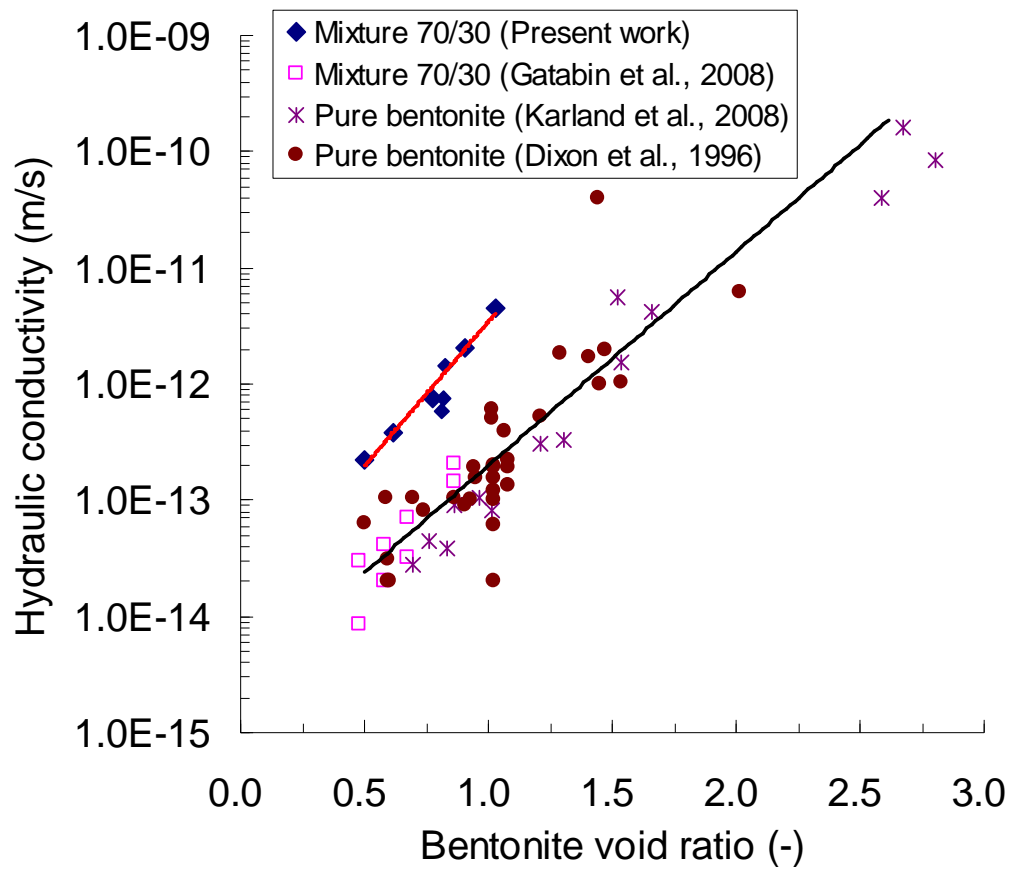


Figure 21. Hydraulic conductivity versus bentonite void ratio



Photo 1. Water outflow through the technological void.